

AN ENERGY CORRECTION ALGORITHM FOR THE OVERLAP REGIONS OF THE ALEPH ELECTROMAGNETIC CALORIMETER

1. Introduction

The electromagnetic calorimeter has a central part made of 12 barrel modules and two end-caps each one composed of 12 petal modules (figure 1). The shape of the modules and the positioning of the central part relatively to the end-caps were designed to have an overlap so that there are no dead angles of detection in that region. The central part and the end-caps are physically separated to allow passage of the ITC and TPC cables and TPC feet. The presence of this dead material leads to energy losses. This note reports of the work done to understand those losses and parametrized them in order to build an energy correction algorithm for the ALEPH reconstruction program JULIA.

2. Description

A particle impinging upon the calorimeter with a polar angle between 37.5° and 44.24° (figure 2) crosses sequentially a barrel module, a region without detector and a petal module. A second overlap region exists for the polar angles between 135.76° and 142.5° . The region between the active volumes of the two modules will be called *dead region* and includes the barrel electronics, the barrel endplate, the region between the two modules and the front plane of the petal. The region between the two modules is filled by 4 different materials (TPC vertical

* Laboratoire de l'Accélérateur Linéaire.

and longitudinal feet, ITC or TPC cables grouped in layers of 8 depending on the azimuthal angle (figure 3) and 4 *types of azimuthal regions* were defined. Because of the projectivity of the calorimeter, five rows of towers of the barrel modules are aligned with five rows of towers of the petal modules; the superposition of one tower of the barrel with one tower of the petal will be called a *supertower*.

The characteristics of the different materials are summarized in table 1. Due to the fact that the characteristics of the materials in the dead region are different from those of the calorimeter lead, a change of behavior of the electromagnetic shower is expected. Mainly the number of radiation lengths in the dead region is lower so that photons will interact softly while the electrons will interact by dE/dx . This will result in a change of the ratio :

$$\frac{\text{number of photons}}{\text{number of electrons}}$$

in the dead region. The second remark concerning the characteristics of the materials is that the calorimeter contains only $16 X_0$ in the overlap region of the towers which is not enough to detect the tail of the electromagnetic shower. So in addition to the energy losses in the dead region, there is leakage through the rear.

3. Available data

Two types of data were available in order to study energy losses in the overlap regions: test data and simulated data.

The test data were taken at CERN from the 09/09/87 to the 14/09/87. One barrel module and one petal module were relatively positioned to reproduce the ALEPH configuration. The modules were hit by a beam of electrons. Three parameters were chosen :

- the electron energy : 3, 10 and 30 GeV;
- the electron polar incident angle : 11 values were tested to scan all the overlap region;
- the material between the two modules :
 - 1 layer of TPC cables;
 - 4 layers of TPC cables;
 - 8 layers of TPC cables;
 - 1 layer of TPC cables and TPC horizontal foot.

An event selection was performed, mainly to have a good spatial and energy definition; the main problem found was due to Bremstrahlung (reference 1).

The second type of data were simulated using GEANT and EGS. An interface with the detector simulation was made to get the test configuration (different materials between the two modules, no detector before the electromagnetic calorimeter).

4. Energy losses and resolution

a) Energy losses

As the electron incident angle varies across the overlapping region of tower's the number of radiation lengths is almost flat so the relative energy loss by leakage through the rear is expected to be constant. Thus the variation of the detected energy with the cluster polar barycenter is mainly due to losses in the dead region. As the incident polar angle varies, the dead region is differently positioned relatively to the shower longitudinal profile, giving different values of detected energies (figure 4). The minimum of energy is detected when the dead region coincides with the maximum of the longitudinal profile of the shower.

Looking at the same curve for different incident energies (figure 4), we observe that the angle, which the minimum of energy is detected for, varies with the incident energy. For an electron of 3 GeV, the maximum of the longitudinal profile occurs after $4.4 X_0$ corresponding to a polar incident angle in the tower number 52 in the barrel module (figure 5). For an electron of 30 GeV, the maximum occurs after $6.9 X_0$ corresponding to a polar incident angle in the tower number 53 in the barrel module. This points out that the energy losses in the dead region varies mainly with the relative position of the dead region and of the maximum of the longitudinal profile of the electromagnetic shower.

The variation of the detected energy with the incident angle for different numbers of layers of TPC cables are showed on figure 6.

We notice the good agreement between test and simulated data.

b) Resolution

The variation of the resolution with the incident angle is showed on figure 7. It grows up to 33%. For the minimum of detected energy there is an improvement due to the equality of the losses in the two supertowers besides the central one.

5. Leakage through the rear and losses in the dead region

The goal of this section is to separate the two sources of energy losses in the overlap region of the electromagnetic calorimeter. We will start with an estimation of the leakage through the rear.

a) Estimation of the leakage through the rear

The method of fitting the experimental longitudinal profile by a parameterized one is not obvious. On one hand, the experimental profile is made of two pieces, one in the barrel and one in the petal which have to be joined. On the other hand, the different characteristics of the lead of the calorimeter and of the materials of the dead region results in a change of the ratio of the numbers of electrons and photons. After the dead region, a few radiation lengths in the calorimeter are necessary to reconstitute the equilibrium and the shape of the electromagnetic shower is changed.

In order to estimate the leakage through the rear, we used a parametrized profile developed in lead (reference 2) and have accounted for the presence of the dead region by its number of radiation lengths.

This last point was checked by comparing the experimental longitudinal profiles (figure 8) induced by electrons of 30 GeV in the overlap region for 1 and 8 layers of TPC cables, at different levels of developments; The results are summarized in table 2. There is a shift of .8 planes corresponding to $.5 X_0$ in the lead. The difference of numbers of radiation lengths between 1 and 8 layers of TPC cables is $.6 X_0$, in agreement with the shift observed. Thus it is possible to take into account the dead region by its number of radiation lengths.

In order to have an estimation of the leakage through the rear, we compared the results given by three different methods : profile developed in the calorimeter, simulation and parametrized profile. The good agreement between the results (table 3) allows an estimation by the parametrized profile. This depends on the numbers of radiation lengths present in the calorimeter which is determined by the polar position of the electromagnetic cluster and on the number of radiation lengths present in the dead region which is determined by the type of azimuthal region through the azimuthal position of the electromagnetic cluster. Finally, the estimation depends on the incident energy which is not measured and will be replaced by another parameter for the correction.

The corrective coefficient C^L is defined by the expression :

$$E = C^L (E - L)$$

where E is the incident energy of the electron and
 L is the leakage through the rear.

The values of the corrective coefficients C^L for the test configuration are given in table 4 and 5.

b) Parametrization of the losses in the dead region

It appeared in section 3 that the detected energy was mainly varying with the relative position of the dead region and of the longitudinal profile of the electromagnetic shower. this relative position is expressed by the ratio :

$$\rho = \frac{B}{B + P}$$

where B is the energy measured in the barrel module and

P is the energy measured in the petal module.

The corrective coefficient C^O of the losses in the dead region are defined by :

$$E = C^L C^O (B + P)$$

The variation of the corrective coefficient C^O with ρ is plotted on figure 9 for 1 and 8 layers of TPC cables for different incident energies and angles. Figure 10 represents C^O as a function of ρ for different materials between the two modules.

Note that, although the estimation of the leakage through the rear can be made taking into account by its number of radiation lengths the dead region, the calculation of the losses in the dead region using a longitudinal profile developed in lead does not give results in agreement with the data.

6. Correction by supertowers

The corrective coefficients C^L and C^O are defined for the whole electromagnetic cluster so the correction would depend on the reconstruction algorithm of the electromagnetic cluster. It would be more satisfying to be independant of the cluster algorithm and apply to each supertower a corrective coefficient . The energy E of the cluster would be then :

$$E = \sum_{ij \text{ of the cluster}} C_{ij}^L C_{ij}^O (B + P)_{ij}$$

where i and j are the polar and azimuthal numbers of the supertower,

$(B+P)_{ij}$ is the energy measured in the supertower,

$C_{i,j}^L$ is the corrective coefficient of the leakage through the rear for the supertower and

$C_{i,j}^O$ is the corrective coefficient of the energy losses in the dead region for the supertower.

In order to test the possibilities of such a correction, we supposed that:

- $C_{i,j}^L$ is equal to the corrective coefficient C^L if the cluster was centered on the supertower i,j

and

- $C_{i,j}^O$ depends on the j that indicates the material present between the two modules and on the ratio :

$$\rho_{ij} = \left(\frac{B}{B + P} \right)_{ij}$$

for the supertower.

a) Data for 1 and 8 layers of TPC cables

The test was made on the data with 1 and 8 layers of TPC cables separately. The values of $C_{i,j}^L$ are extracted from tables 4 and 5. The values of $C_{i,j}^O$ are obtained by iteratively adjusting the corrected energy of the cluster to the nominal value of the electron energy for all the incident angles and all the incident energies of the tests. The curve $C_{i,j}^O = f(\rho_{i,j})$ is given in 21 points and the intermediate values are obtained by a linear interpolation. The variation of $C_{i,j}^O$ with $\rho_{i,j}$ and of the corrected energy of the cluster with ρ are showed on figure 11 for 1 layer of TPC cables and on figure 12 for 8 layers of TPC cables. The energy is corrected by up to 7%. In addition, the resolution is noticeably improved (figure 13).

b) Data for 4 layers of TPC cables

Instead of making an iteration to get the corrective coefficient $C_{i,j}^{O,4}$ for the 4 layers of TPC cables, they are obtained by interpolation of the corrective coefficient $C_{i,j}^{O,1}$ and $C_{i,j}^{O,8}$ for the 1 and 8 layers configuration. For each of the 21 points of the curve the corrective coefficient $C_{i,j}^{O,4}$ is calculated through the expression:

$$C_{ij}^{O,4} = C_{ij}^{O,1} + \frac{4-1}{8-1} (C_{ij}^{O,8} - C_{ij}^{O,1})$$

The variation of $C_{i,j}^O$ with $\rho_{i,j}$ and of the corrected energy of the cluster with ρ are showed on figure 14. The energy is corrected up to 5%.

7. An algorithm of energy correction

This algorithm is based on the correction by supertowers, previously tested. The energy of the cluster is :

$$E = \sum_{ij \text{ of the cluster}} C_{ij}^L C_{ij}^O (B + P)_{ij}$$

where i and j are the polar and azimuthal numbers of the supertower,

C_{ij}^L is the corrective coefficient of the leakage through the rear for the supertower

and

C_{ij}^O is the corrective coefficient of the energy losses in the dead region for the supertower.

a) Correction of the losses in the dead region

Instead of taking the ratio $\rho_{i,j}$ it is more convenient to sum over the j of the cluster to avoid problems in case of an electron, deviated in the magnetic field. So we will consider the ratio :

$$\rho_i = \frac{\sum_{j \text{ of the cluster}} B_{i,j}}{\sum_{j \text{ of the cluster}} (B + P)_{i,j}}$$

The corrective coefficient depends on :

- the ratio ρ_i ,
- the number j of the supertower which determines the type of azimuthal region through the material present between the two modules.

From the type of azimuthal region, we can deduce which of the curves, out of the four, we have to take. These curves are given in 21 points (table 6) and the intermediate values are obtained by a linear interpolation. The value of ρ_i gives the corrective coefficient $C_{i,j}^O$.

For the untested configuration with only air between the two modules, it was assumed to be equivalent to 0 layer of TPC cables and the corrective coefficients $C_{i,j}^O$ were extrapolated from the data at 1 and 8 layers of TPC cables. For the configurations with TPC feet, the corrective coefficients C^O for the cluster were compared to the one for 1 and 8 layers of TPC cables and the proportionality was used to get the corrective coefficients $C_{i,j}^O$ for the supertower.

b) Correction of the leakage through the rear

Until now, the energy correction was depending on the nominal energy of the electron which is not measured and so we have to change this parameter. The energy measured in a supertower is interesting because it does not depend on the cluster reconstruction but is not sensitive of the leakage through the rear. Taking the energy of the whole cluster is also meaningless in the case of a π^0 that has decayed into two photons. The intermediate solution is to look for maxima in the cluster, build an area of 2 by 2 supertowers around each maximum and consider the energy deposited in those areas. We define :

$$E_4 = \sum_{4 \text{ supertowers}} C_{ij}^O (B+P)_{ij}$$

The ratio:

$$r = \frac{E_4}{E}$$

has been studied (reference 3) and the results of the test beam and simulated data are showed on table 7 and 8. We took the value $r = 87.\%$. The energy E_4 corrected by r is the energy of the cluster.

The corrective coefficient C_{ij}^L depends thus on :

- the number j which determines the number RL_1 of radiation lengths between the two modules,
- the number i which determines the number RL_2 of radiation lengths in the calorimeter ,
- the energy E_4 .

These parameters allow to calculate the value of τ :

$$\tau = \frac{(RL_1 + RL_2)}{1.08 \text{ Log} \frac{E_4}{0.05}}$$

from which it is possible to deduce the corrective coefficient through the table 9.

8. Conclusion

In a first approach, it was showed that it is possible to correct the measured energy using two multiplicative factors :

- C^O correcting the losses in the dead region and depending only on the ratio ρ for a particular material between the two modules,
- C^L correcting the leakage through the rear.

A correction by supertower was also tested where th energy is corrected by up to 7% and a significant improvment of the resolution is seen.

An algorithm of correction has been developped and is being implemented in JULIA.

9. Acknowledgements

We are very gratefull to J.Lefrancois for discussions that help the understanding of physical phenomena and the building of the correction algorithm. We are very thankfull to B.BLoch who made corrections to get the test configuration in GALEPH.

References

- reference 1 : V.P. Marotte, these de doctorat en science physique, LAL 89-17
reference 2 : E.Longo and I.Sestili, Nuclear Instruments and Methods in Physics Research
128(1975)283-307
reference 3 : Pallin, private communication

Tables :

- table 1 : Characteristics of the materials in the overlap region
table 2 : Comparison of the longitudinal development of showers induced by electrons
of 30 GeV in the overlap region for 1 or 8 layers of TPC cables
table 3 : Comparison of the leakage through the rear estimated by different methods (30 GeV)
table 4 : Corrective coefficient C^L for 8 layers of TPC cables
table 5 : Corrective coefficient C^L for 1 layer of TPC cables
table 6 : Corrective coefficient $C_{i,j}^O$ for the different azimuthal regions
table 7 : Ratio r from the test data
table 8 : Ratio r from the simulated data
table 9 : Corrective coefficient $C_{i,j}^L$ as a function of τ

Figure captations

- figure 1 : Central part and end-caps of the electromagnetic calorimeter
- figure 2 : Longitudinal cross-section of one of the overlap regions of the electromagnetic calorimeter
- figure 3 : Transversal cross-section
- figure 4 : Variation of the measured energy with the cluster polar barycenter for different incident energies
- figure 5 : Longitudinal profile for electrons of 3 and 30 GeV and polar incident angle for which the energy loss is maximum
- figure 6 : Variation of the measured energy with the cluster polar barycenter for different numbers of layers of TPC cables
- figure 7 : Variation of the resolution with the cluster polar barycenter
- figure 8 : Experimental longitudinal profiles for electrons of 30 GeV incoming in the overlap region
- figure 9 : Variation of the corrective coefficient C^O with ρ for 1 and 8 layers of TPC cables
- figure 10 : Variation of the corrective coefficient C^O with ρ for different materials between the two modules
- figure 11 : Correction by supertowers for 1 layer of TPC cables
- a) variation of the corrective coefficient $C_{i,j}^O$ with the ratio $\rho_{i,j}$
 - b) variation of the relative corrected energy with the ratio ρ
- figure 12 : Correction by supertowers for 8 layers of TPC cables
- a) variation of the corrective coefficient $C_{i,j}^O$ with the ratio $\rho_{i,j}$
 - b) variation of the relative corrected energy with the ratio ρ
- figure 13 : Variation of the resolution with the cluster polar barycenter for corrected data
- figure 14 : Correction by supertowers for 4 layers of TPC cables
- a) variation of the corrective coefficient $C_{i,j}^O$ with the ratio $\rho_{i,j}$
 - b) variation of the relative corrected energy with the ratio ρ

characteristics materials	lentgh (cm)		thickness		
	R	z	cm	rad. lengths	g/cm ² corrected by Z/A
<i>Barrel</i>					
front plane	184.69		2.1	0.213	2.472
stack 1	186.79		7.83	3.83	11.512
PVC	194.62		0.5	0.027	0.334
stack 2	195.12		18.01	8.813	26.478
PVC	213.13		0.5	0.027	0.334
stack 3	213.63		11.80	8.869	24.629
	225.43				
passive volume		231.5	4.6	.119	1.980
endplate		236.1	2.6	.281	3.383
		238.7			
8 layers of ITC or TPC cables		240.0	8.8	.522	6.225
		248.8			
TPC horizontal foot		240.0	8.5	0.188	2.166
		248.5			
TPC vertical foot		240.0	8.5	0.708	6.616
		248.5			
<i>Petal</i>					
front plane		252.1	2.1	0.194	2.383
stack 1		254.2	8.62	3.615	11.749
aluminium		262.82	0.63	0.071	0.826
stack 2		263.45	19.83	9.107	28.486
aluminium		283.28	0.63	0.071	0.826
stack 3		296.66	12.74	9.038	25.734

table 1

	1 layer of TPC cables	8 layers of TPC cables
maximum	5.5 - 6 th plane	5. - 5.5 th plane
20 % of maximum	14.4 th plane	13.5 th plane
half-maximum	19.5 th plane	19.7 th plane

table 2

	experimental profile	paramatrized profile	simulation
1 layer of TPC cables	7.3%	7.0%	7.3%
8 layers of TPC cables	5.9%	5.7%	6.0%

table 3

tower polar number		number of radiation lentghs	electron of 30 GeV	electron of 10 GeV
barrel module	petal module			
	44	20	1.013	1
	45	16.4	1.056	1.017
51	46	15.9	1.071	1.021
52	47	"	"	"
53	48	"	"	"
54	49	"	"	"
55	50	16.9	1.056	1.013
56		18.6	1.027	1
57		19.8	1.015	1

table 4

tower polar number		number of radiation lentghs	electron of 30 GeV	electron of 10 GeV
barrel module	petal module			
	44	20	1.013	1
	45	16.4	1.056	1.017
51	46	16.5	1.056	1.017
52	47	"	"	"
53	48	"	"	"
54	49	"	"	"
55	50	17.5	1.042	1.010
56		18.6	1.027	1
57		19.8	1.015	1

table 5

type of azimuthal region ratio $\rho_{i,j}$	1 air	2 8 layers of TPC cables	3 TPC horizontal foot	4 TPC vertical foot
0.	1.	1.	1.	1.
0.05	1.13	1.18	1.12	1.3
0.1	1.20	1.26	1.19	1.37
0.15	1.24	1.32	1.24	1.43
0.2	1.28	1.38	1.26	1.48
0.25	1.30	1.43	1.28	1.52
0.3	1.33	1.47	1.31	1.54
0.35	1.36	1.49	1.33	1.55
0.4	1.37	1.50	1.34	1.56
0.45	1.38	1.51	1.34	1.57
0.5	1.38	1.51	1.34	1.57
0.55	1.38	1.51	1.34	1.57
0.6	1.37	1.50	1.34	1.56
0.65	1.36	1.49	1.33	1.55
0.7	1.33	1.47	1.31	1.54
0.75	1.30	1.43	1.28	1.52
0.8	1.28	1.38	1.26	1.48
0.85	1.24	1.32	1.24	1.43
0.9	1.20	1.26	1.19	1.37
0.95	1.13	1.18	1.12	1.3
1.	1.	1.	1.	1.

table 6

E (GeV)	E4/E (%)
50	86.1 + - .2
25	86.8 + - .2
10	88.1 + - .2
5	90.1 + - .3
2	92.7 + - .3
1	96.0 + - .5

table 7

E (GeV)	E4/E (%)
50	87.1 + - .3
25	87.2 + - .2
10	88.0 + - .4

table 8

τ	CL
0.05	216.0
0.15	66.
0.25	31.
0.35	17.
0.45	11.
0.55	7.
0.65	5.
0.75	4.
0.85	3.
0.95	2.6
1.05	2.2
1.15	1.97
1.25	1.76
1.35	1.61
1.45	1.49
1.55	1.40
1.65	1.33
1.75	1.21

τ	CL
1.85	1.22
1.95	1.18
2.05	1.15
2.15	1.12
2.25	1.10
2.35	1.08
2.45	1.0
2.55	1.06
2.65	1.04
2.75	1.03
2.85	1.03
2.95	1.02
3.05	1.02
3.15	1.02
3.25	1.01
3.75	1.01
4.05	1.

table 9

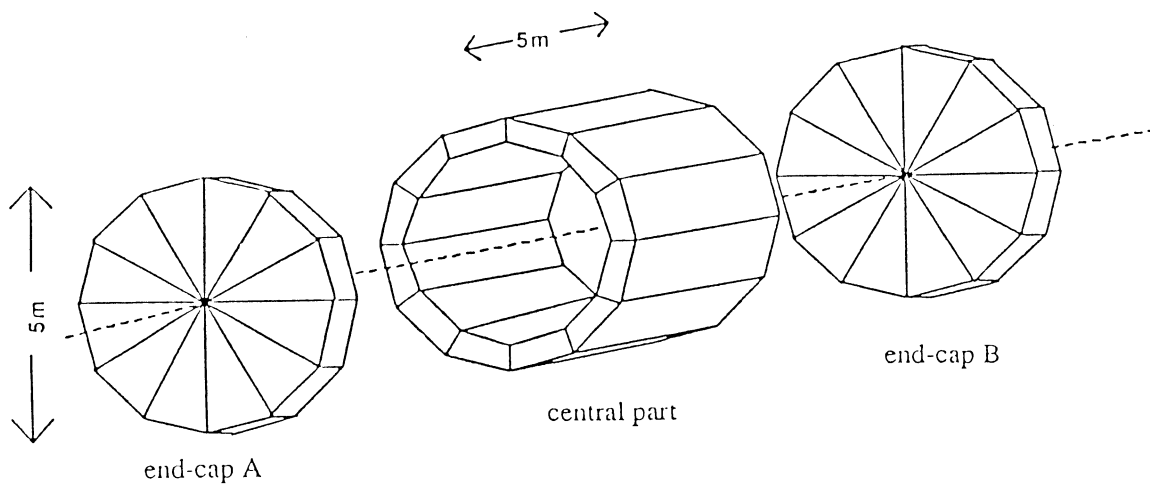
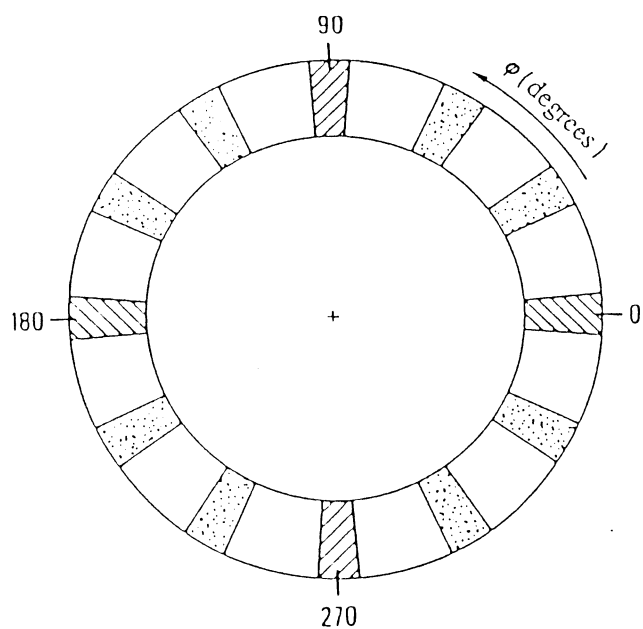
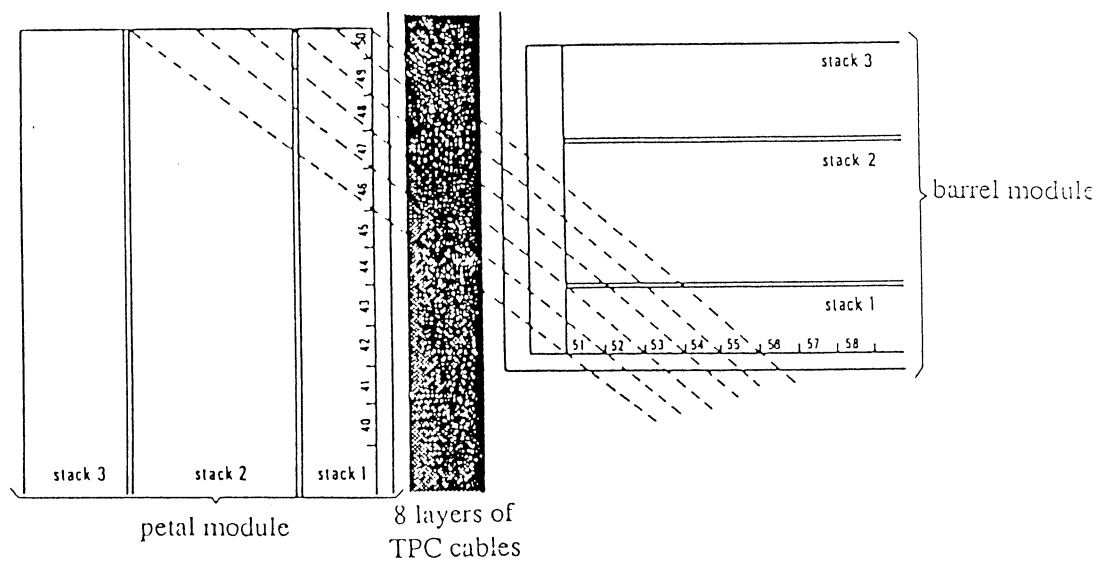


figure 1

figure 2



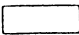
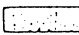

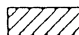
-  azimuthal region of type 1 :
air only
-  azimuthal region of type 2 :
8 layers of TPC or ITC cables
-  azimuthal region of type 3 :
TPC horizontal foot
-  azimuthal region of type 4 :
TPC vertical foot

figure 3

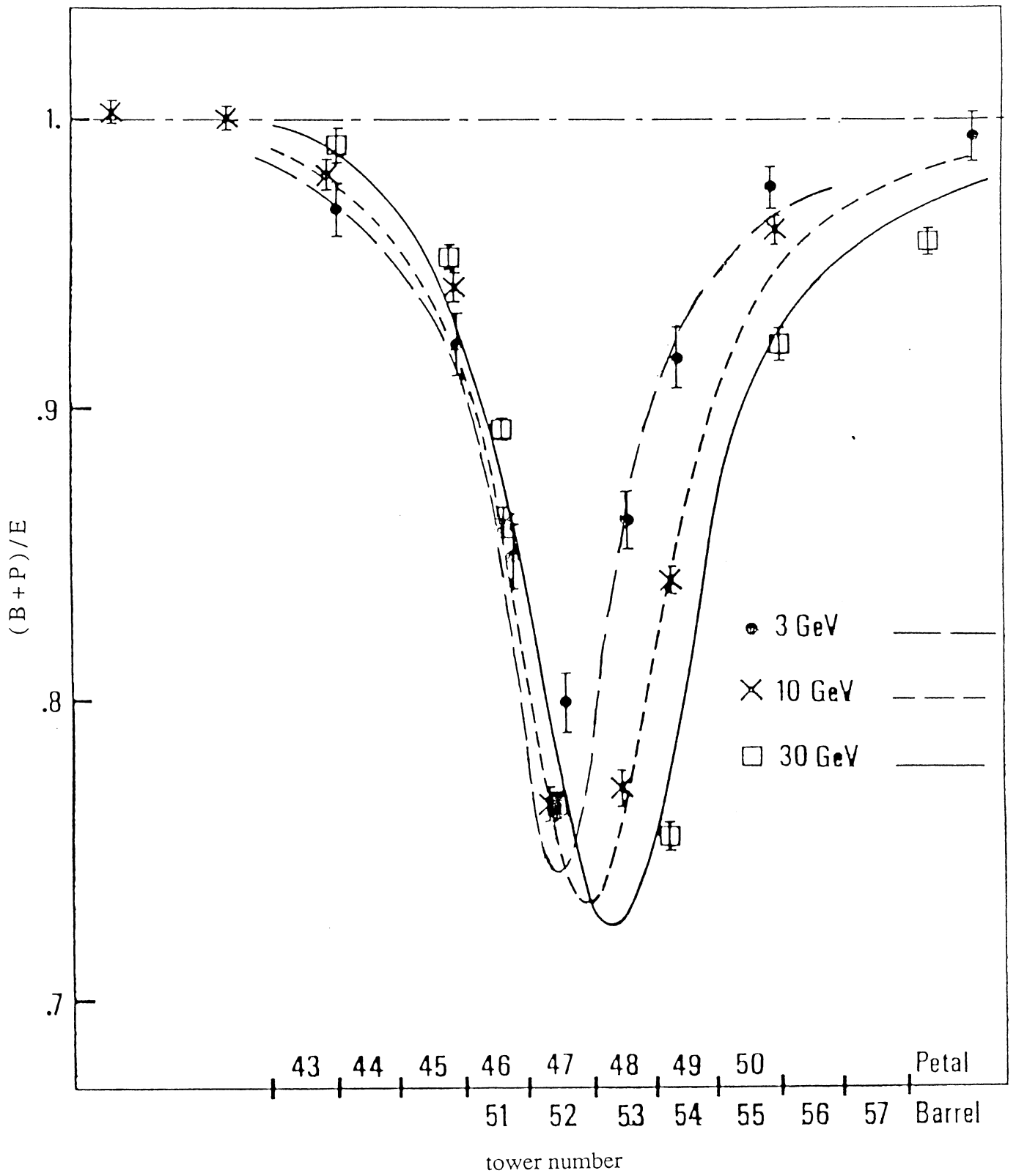


figure 4

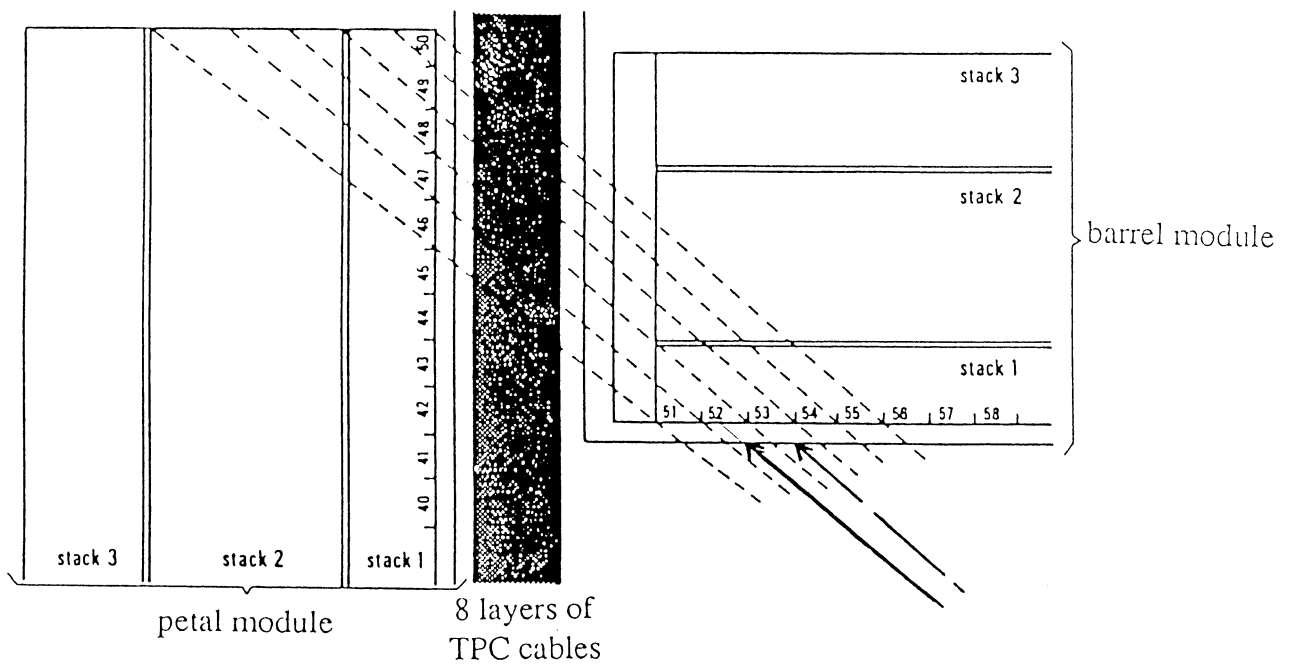
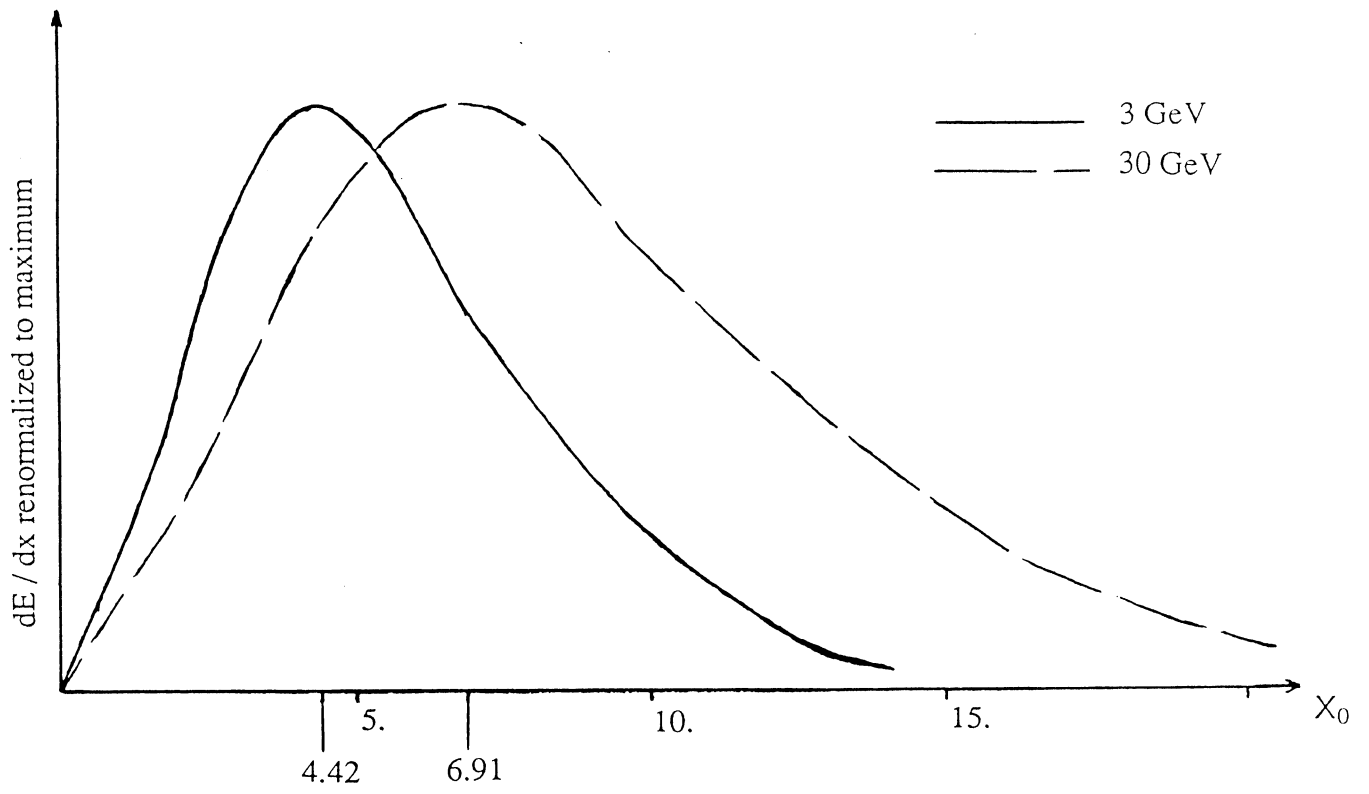


figure 5

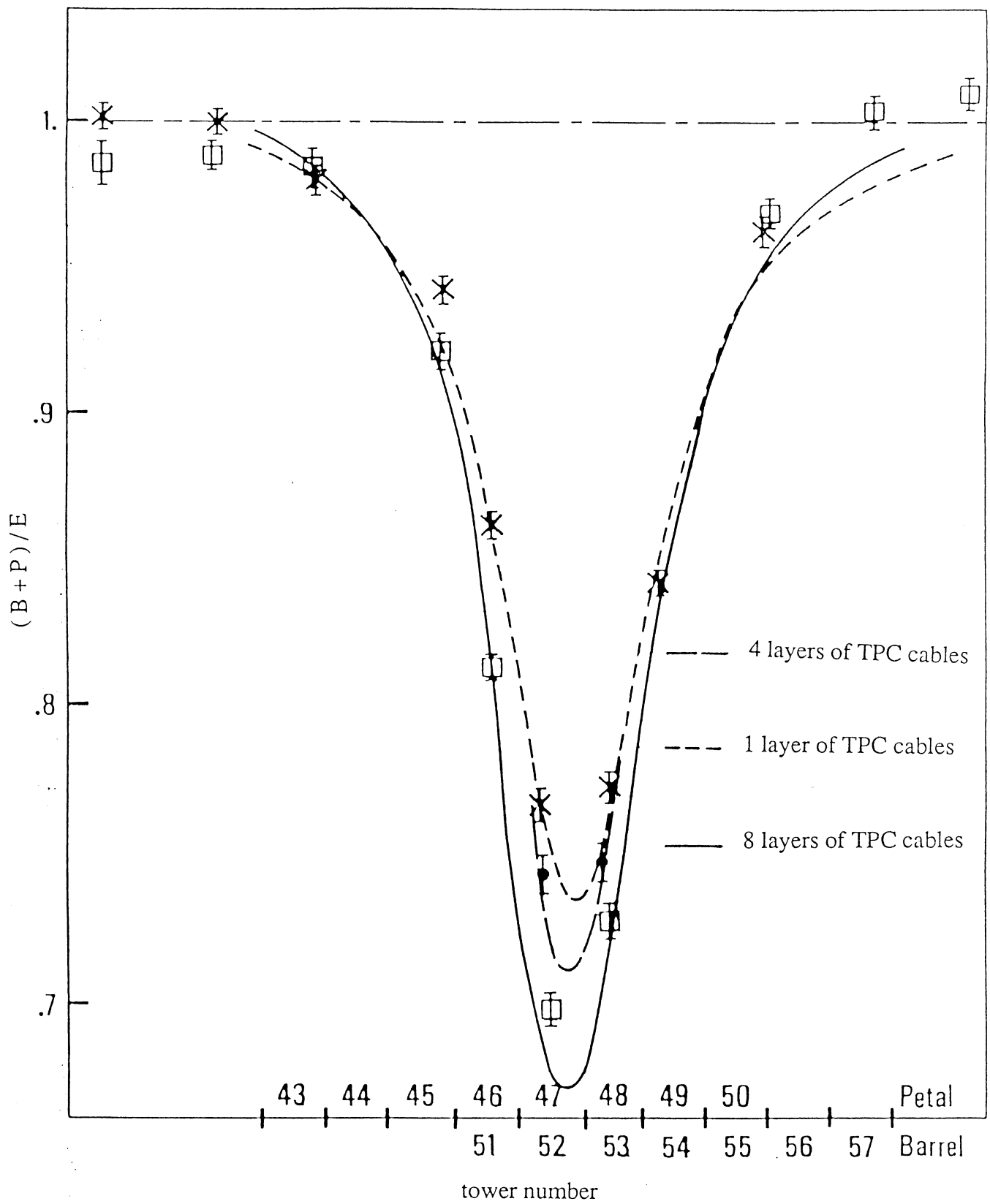


figure 6

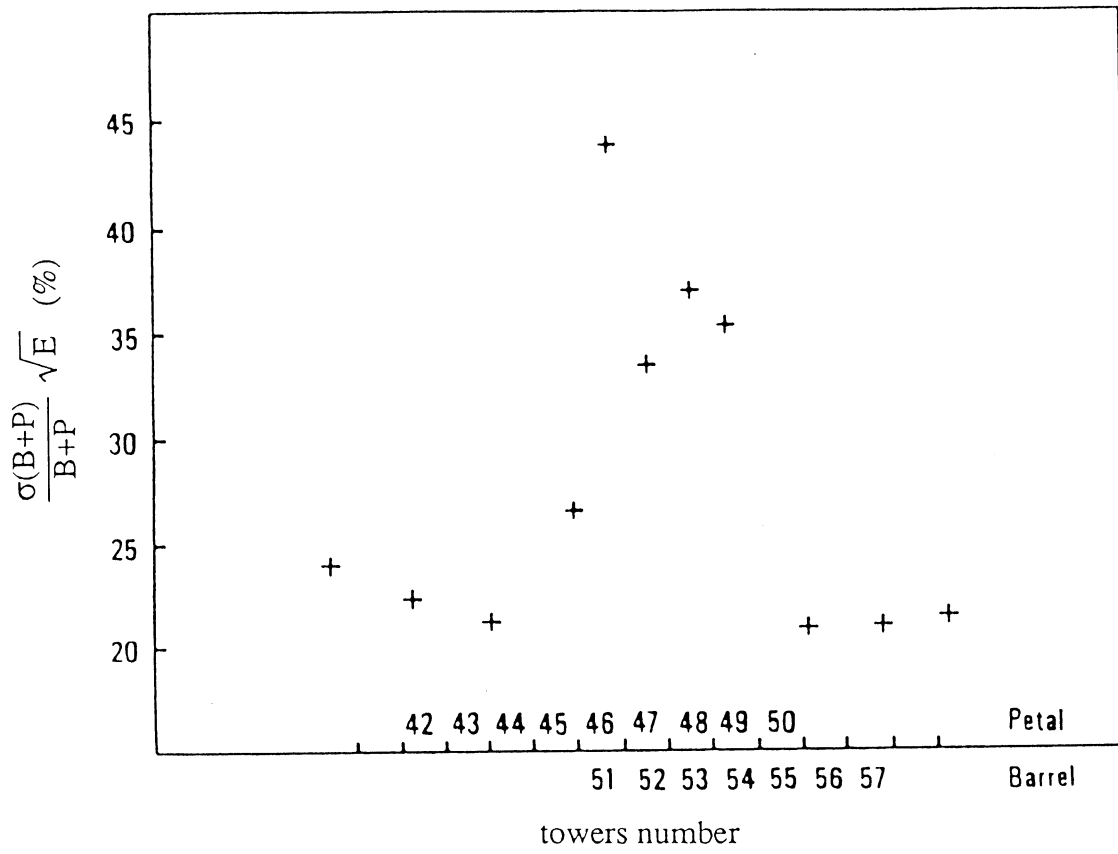


figure 7

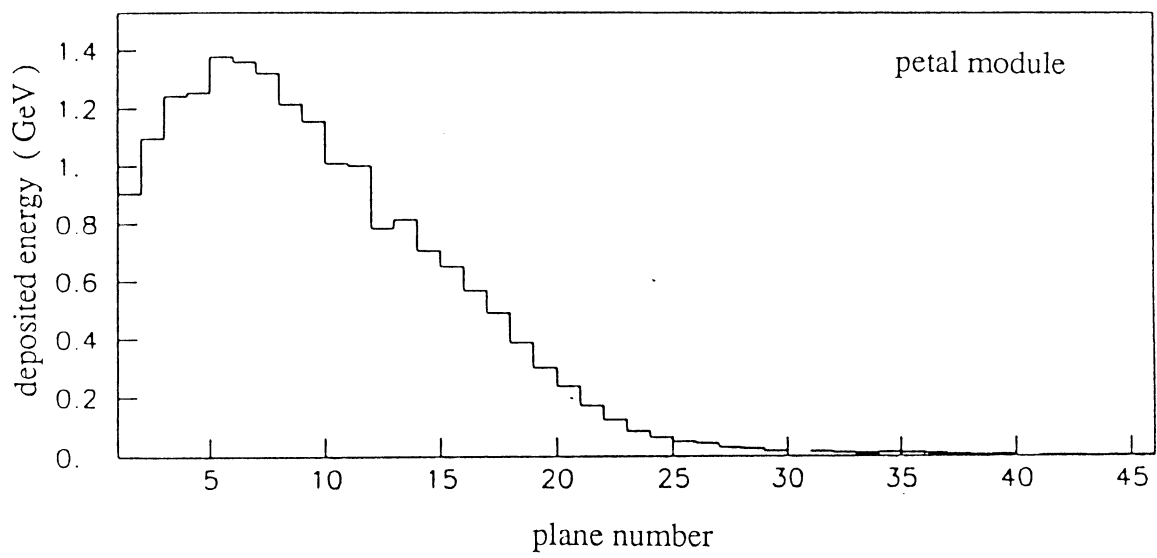
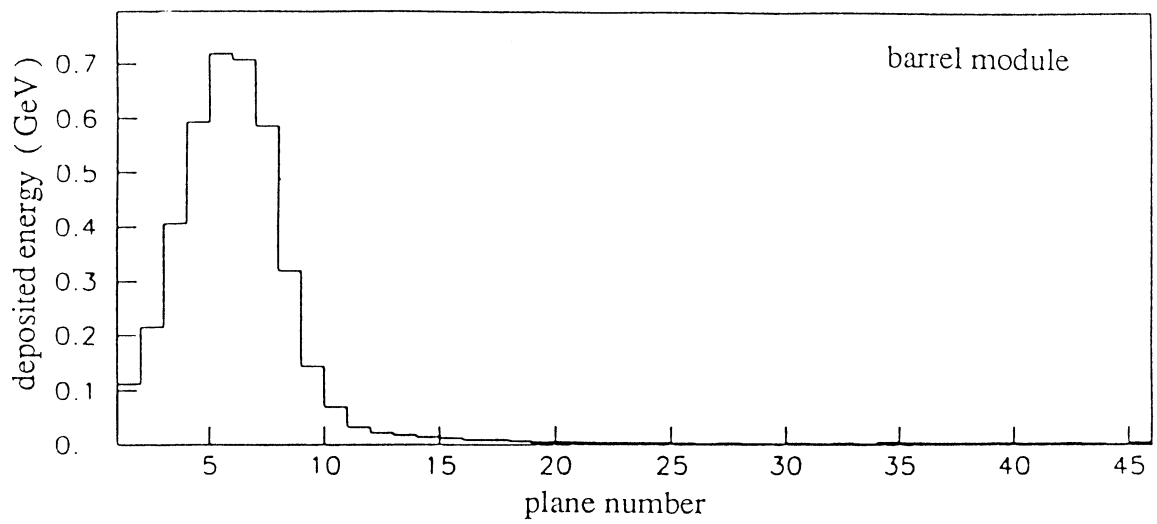


figure 8

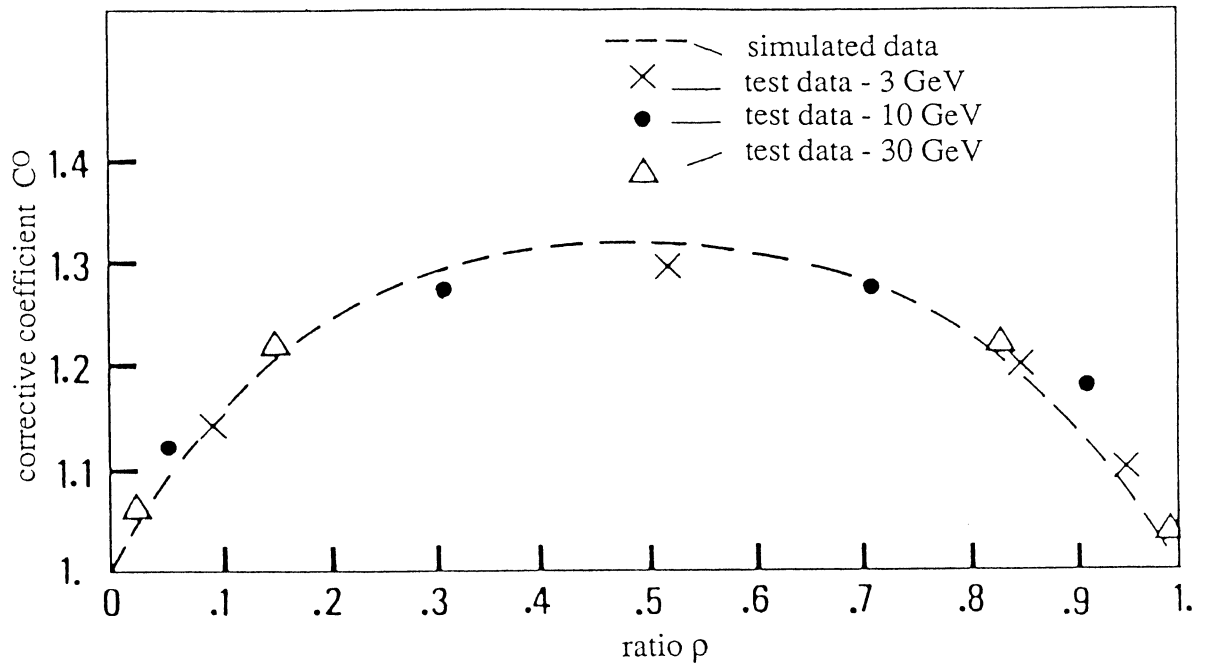


figure 9

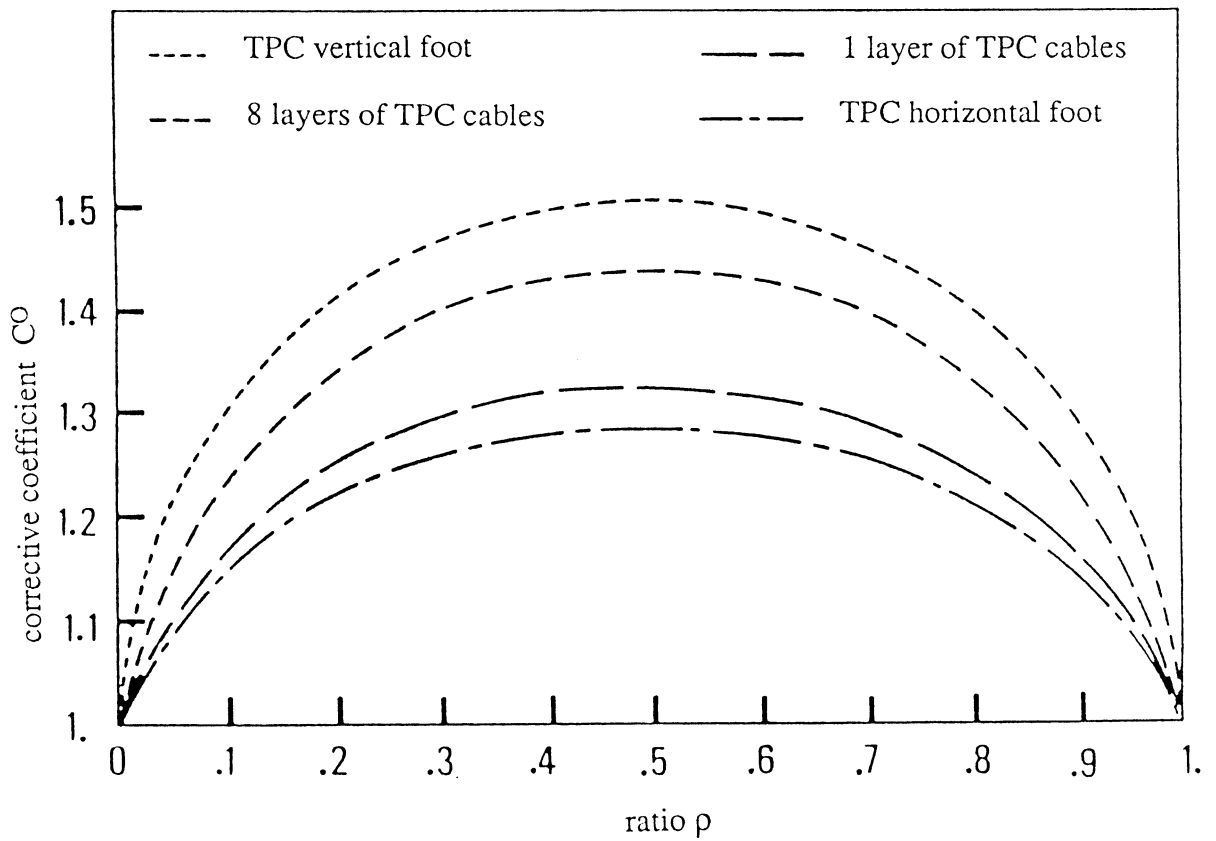


figure 10

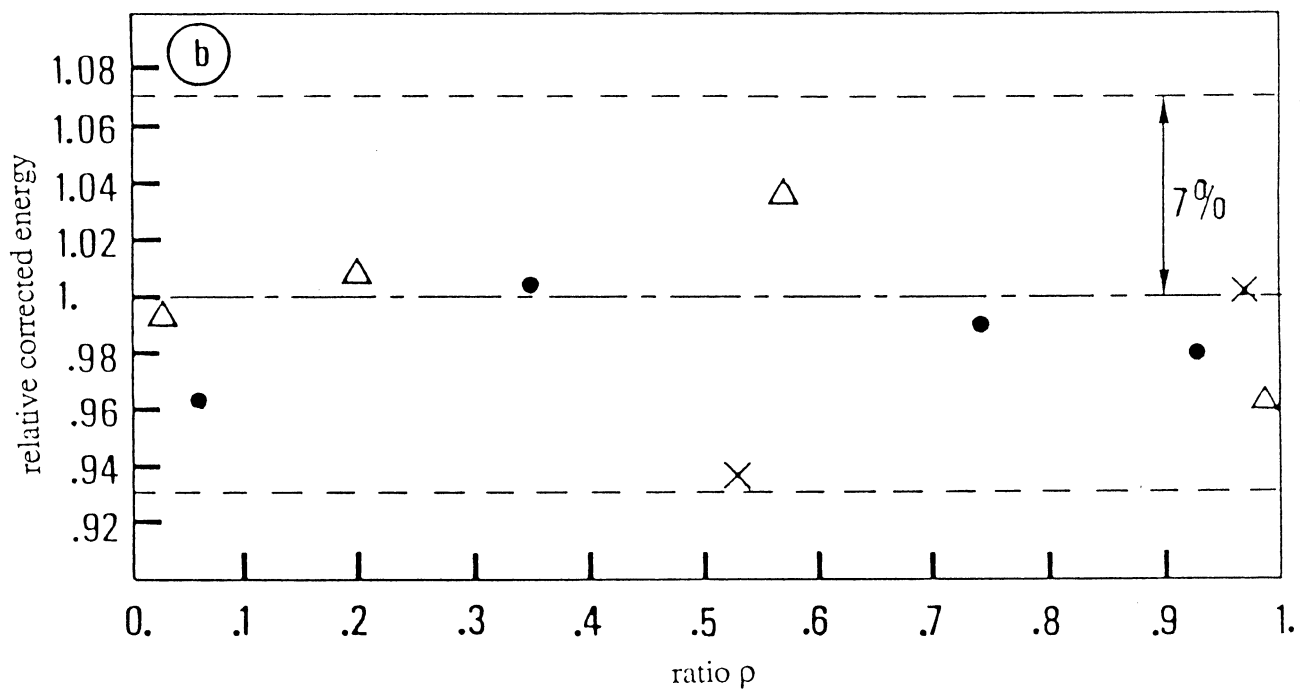
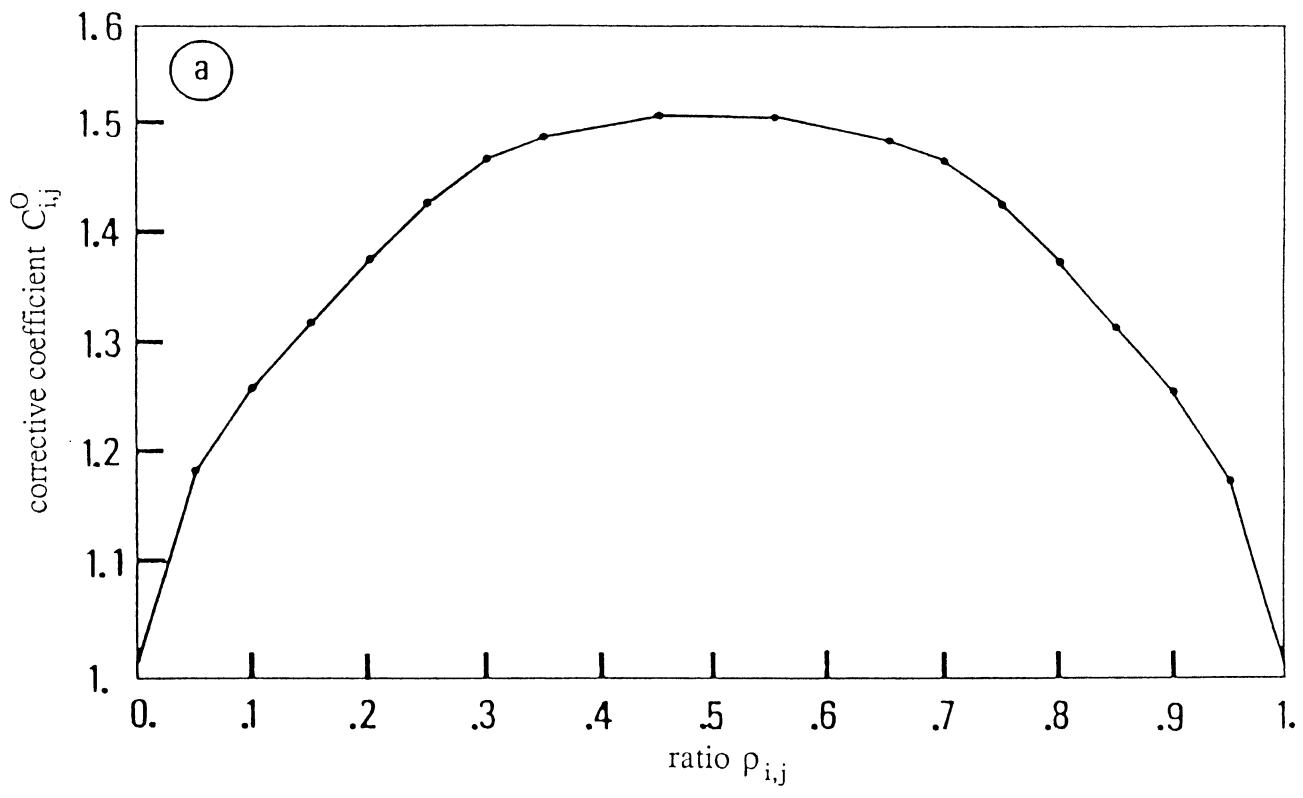


figure 12

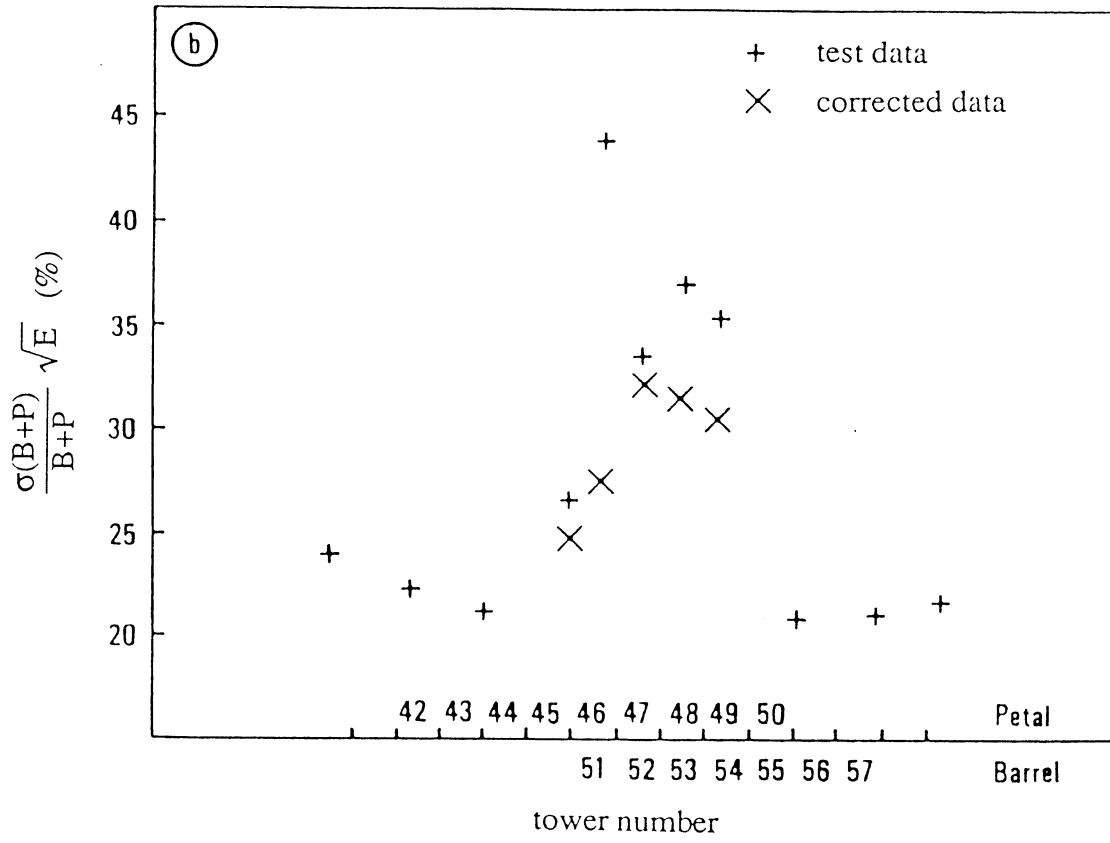


figure 13

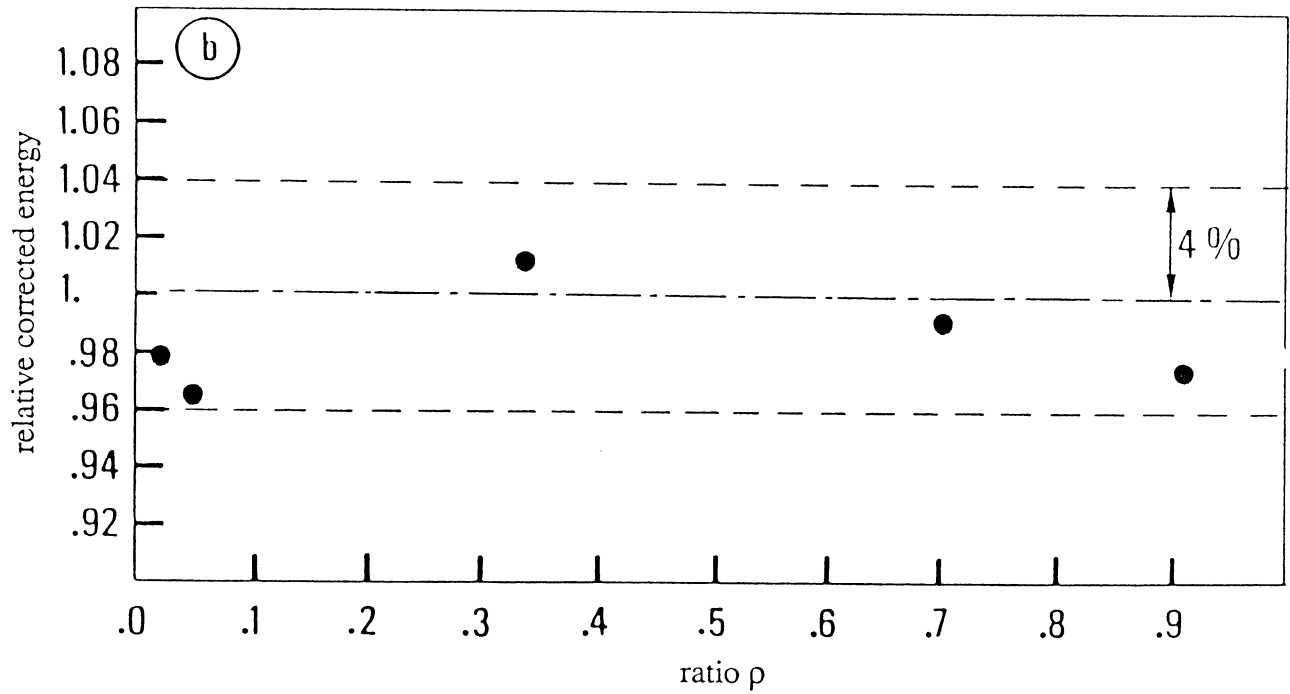
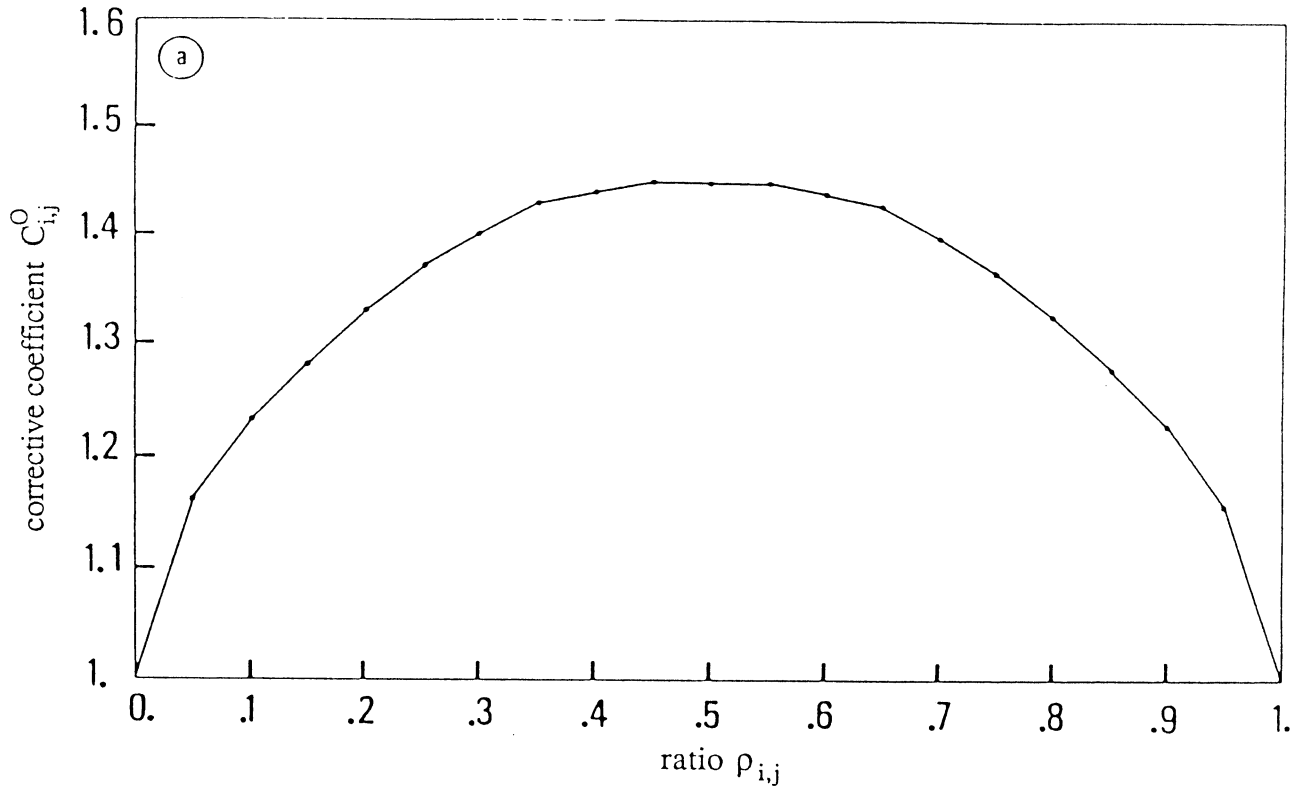


figure 14